Applied Clay Science 50 (2010) 546–553

Contents lists available at ScienceDirect

Applied Clay Science

journal homepage: www.elsevier.com/locate/clay

Influences of thermal pretreatment temperature and solvent on the organosilane modification of Al_{13}-intercalated/Al-pillared montmorillonite

Zonghua Qin [a,b], Peng Yuan [a,*], Jianxi Zhu [a], Hongping He [a], Dong Liu [a,b], Shuqin Yang [a,b]

[a] Guangzhou Institute of Geochemistry, Chinese Academy of Sciences, Guangzhou 510640, PR China
[b] Graduate School of Chinese Academy of Sciences, Beijing 100049, PR China

ARTICLE INFO

Article history:
Received 26 July 2010
Received in revised form 12 October 2010
Accepted 12 October 2010
Available online 20 October 2010

Keywords:
3-Aminopropyltriethoxysilane
Intercalated clay
Pillared clay
Grafting
Thermal treatment
Inorganic–organic hybrid material

ABSTRACT

The grafting reactions between 3-aminopropyltriethoxysilane and Al_{13}-intercalated/Al-pillared montmorillonites thermally pretreated at different temperatures were investigated by using X-ray diffraction, Fourier transform infrared spectroscopy, thermogravimetric analysis, elemental analysis and nitrogen adsorption–desorption isotherms. The porous structures and the grafting degree of the organosilane modified Al_{13}-intercalated/Al-pillared montmorillonite products are significantly affected by the solvents. The product prepared in anhydrous ethanol has high specific surface area (~160 $m^2 g^{-1}$) and larger porous volume (0.134 $cm^3 g^{-1}$) but low degree of grafting modification, while the one prepared in cyclohexane has a high loading amount of silane (2.02 mmol g^{-1}) but low surface area (7 $m^2 g^{-1}$). Thermal treatment affects the grafting process by both reducing the water content in the interlayer space of the pillared montmorillonite and causing the transformation of the interlayer Al compounds from polycations to oxides. The hydrolyzed 3-aminopropyltriethoxysilane is mainly grafted onto the surface of the interlayer Al Keggin ions and/or Al oxides. This study demonstrates the functionalization of pillared clay to form inorganic–organic hybrid material that combines the high porosity of inorganic pillared clay and the lipophilicity of organoclay by adjusting the solvents and the pretreatment conditions, enabling potential applications in adsorption and environmental restoration.

1. Introduction

Pillared interlayered clay (PILC), which had thermal stability, large specific surface area, and micro-/meso-porosity (Kloprogge, 1998; Occelli et al., 2000; Chae et al., 2001; Ding et al., 2001; Yuan et al., 2006), was extensively used as selective absorbents for the removal of heavy metal ions (Bhattacharyya and Sen Gupta, 2008; Wu et al., 2009) and the separation of inorganic gases (Yang and Baksh, 1991; Pires et al., 2008), and catalysts for petroleum refinery (Pinnavaia, 1983; Gonzalez et al., 1999; Martinez-Ortiz et al., 2003) and environmental restoration (Shimizu et al., 2002; Cheng et al., 2008; Chen et al., 2009). PILC was prepared by exchanging the charge-compensating cations between the swelling clay layers with larger polymeric or oligomeric hydroxyl metal cations. Among them, Al-pillared clay, the first prepared inorganic PILC, had attracted great research interests and intensively investigated (Jiang et al., 2002; Itadani et al., 2007). However, the adsorption of organic pollutants on Al-pillared clay is ineffective due to the hydrophilicity of clay surface which was caused by the hydration of inorganic cations on the exchange sites (Tunega et al., 2002; Liu and Lu, 2006; Malani et al., 2009).

In order to enhance the lipophilicity of clay minerals, organoclay was widely studied. They were prepared by surface modification of clay minerals using organic compounds (Bergaya and Lagaly, 2001; Liu, 2007; de Paiva et al., 2008; Zhu et al., 2009b). The most commonly used method to prepare organoclay was the ion exchange of interlayer cations of smectites with cationic surfactants, e.g. quaternary ammonium compounds (Lagaly, 1986; de Paiva et al., 2008). And the adsorptive capacity of organoclay used for removing organic pollutants in water and air was investigated (Baskaralingam et al., 2006; Sanchez-Martin et al., 2006; Xi et al., 2007). Another method for organic modification of clay materials was the functionalization with organosilanes (Carrado et al., 2001; He et al., 2005; Herrera et al., 2004; Wheeler et al., 2005; Yuan et al., 2008). It attracted the researchers' attentions in view of the applications of organo-functionalized clays in polymer-clay nanocomposites recently (Okada and Usuki, 2006). In this method, silanol groups that resulted from the hydrolysis of organosilanes condensed with the hydroxyl groups of the layered silicates, forming stable Si–O–Si covalent bonds (He et al., 2005; Daniel et al., 2008). The silylated clay was further mixed with the polymer to improve the optical, dielectric, thermal, rheology and mechanical properties of the polymer-clay nanocomposites (Ruiz-Hitzky and Meerbeek, 2006). As evident in the previous

* Corresponding author. Guangzhou Institute of Geochemistry, Chinese Academy of Sciences, Wushan, Guangzhou 510640, PR China. Tel.: +86 20 85290341; fax: 86 20 85290130.
E-mail address: yuanpeng@gig.ac.cn (P. Yuan).

0169-1317/$ – see front matter © 2010 Elsevier B.V. All rights reserved.
doi:10.1016/j.clay.2010.10.011

reports (Alkaram et al., 2009), organic modification by surfactant can significantly increased the affinity between clays and organic pollutants, but the interlayer spaces of the clays were mostly occupied by the surfactants (Zhu et al., 2008a; Zhu et al., 2008b) or organosilane species (He et al., 2005) after organic modification, which led to the lack of pore structures. Consequently, there were not sufficient spaces for the organic pollutants to enter into the interlayer spaces of the clays, so that the adsorptive applications of organoclay were highly limited.

In this sense, it should be very interesting to develop novel inorganic–organic hybrid structure combining the high porosity of inorganic pillared clay and the lipophilicity of organoclay. Several attempts have been made for this goal. Zhu et al. (2007) prepared an organo-inorgano composite sorbent by grafting Al-pillared montmorillonite with trimethylchlorosilane (TMCS) and octadecyltrichlorosilane (OTS) and investigated its adsorption capacity for the removal of volatile organic compounds (VOCs). Zhu et al. (2009a) synthesized an inorganic–organic clay, in which both cetyltrimethyl ammonium bromide (CTAB) and hydroxy-aluminum ($[Al_{13}O_4(OH)_{24}(H_2O)_{12}]^{7+}$, Al_{13}) were intercalated into montmorillonite, and discussed its structural characteristics. However, the specific surface areas of these hybrid materials decreased significantly, almost 60% smaller than the unmodified Al-pillared montmorillonite (Zhu et al., 2007), thus the adsorption capacities of these compounds were restricted. Furthermore, the factors that might affect the structures of the final products, e.g. the pretreatment condition of pillared clay and the type of solvents, were less considered in these studies. Accordingly, it is greatly important to study the synthesis of inorganic–organic clay with high specific surface area and porosity, and to investigate the influences of pretreatments and solvents on the structure of the inorganic–organic clay.

In this work, 3-aminopropyltriethoxysilane (APTES) was used for the functionalization of the pristine and calcined Al_{13}-intercalated/Al-pillared montmorillonites in two different solvents (anhydrous ethanol and cyclohexane). The aim of this work was to investigate the preparation method of functionalized Al_{13}-intercalated/Al-pillared montmorillonite with high porosity and determine the factors that affect the final products and their microstructures. All results were obtained by X-ray diffraction (XRD), Fourier transform infrared spectroscopy (FTIR), simultaneous thermogravimetric analysis (TG–DTG), elemental analysis and nitrogen adsorption–desorption isotherms.

2. Experimental

2.1. Materials

The montmorillonite (Mt) used in this study was from Inner Mongolia, China. The cation exchange capacity (CEC) was 106 cmol(+) kg^{-1}. The chemical compositions (wt.%) of Mt were: SiO_2 49.44%, Al_2O_3 15.94%, Fe_2O_3 2.47%, CaO 4.36%, MgO 4.02%, K_2O 0.13%, Na_2O 0.52%, MnO 0.015%, TiO_2 0.31%, P_2O_5 0.067%, and the ignition loss was 22.55%. The clay was used without further purification. 3-Aminopropyltriethoxysilane (APTES) with a purity of 99% was supplied by Sigma-Aldrich, Inc. All chemicals and reagents used in this work were of analytical grade and used as received.

2.2. Synthesis of Al_{13}-intercalated/Al-pillared montmorillonite and its thermally treated derivatives

2.0 mol L^{-1} Na_2CO_3 solution was slowly added into 0.5 mol L^{-1} $AlCl_3$ solution with continuous stirring under water bath at 60 °C, keeping the final ratio of $[OH^-]/[Al^{3+}]$ to 2.4:1. After that, stirring was needed for another 2 h. Then the solution was aged for 24 h at 60 °C.

Montmorillonite powder was added into the above-mentioned solution, and the mass ratio of solid/liquid is 1:10. The mixture was stirred for 12 h at 60 °C, and stirred for an additional 12 h without water bath. The product was deposited for 9 h, dumping the supernatant. The solid at the bottom was washed by distilled water following a centrifugation at 3000 revolutions per minute (rpm) for 5 min, and this step was repeated 6 times. The precipitate was oven dried at 60 °C, then ground into powder and sealed, finally placed into a desiccator. This intercalated sample was denoted as Al_{13}-IMt.

Al_{13}-IMt samples were calcinated at 300 and 500 °C for 8 h, respectively. And the calcinates were cooled at a desiccator. These pillared samples were denoted as AlPMt-300 and AlPMt-500.

2.3. Methods of organosilane modification

10 g of the intercalated and/or pillared clays was added into 200 ml anhydrous ethanol in a flask. And the mixture was treated by ultrasound at 60 °C for 10 min. 5 ml APTES was added into the mixture under a fast stirring. The suspension was refluxed at 80 °C for 20 h under stirring of 400 rpm. The products were washed 6 times with anhydrous ethanol by centrifugation. The solids were oven dried at 80 °C, ground and sealed in polyethylene bottles. According to the raw materials and the solvent, the final powders were denoted as Al_{13}-IMt/E, AlPMt-300/E, and AlPMt-500/E, respectively.

Following the same procedures mentioned earlier and using cyclohexane to replace anhydrous ethanol, the final samples were denoted as Al_{13}-IMt/C, AlPMt-300/C, and AlPMt-500/C.

2.4. Characterization methods

The basal spacings of these powders were determined by XRD using a Brucker D8 advanced diffractometer equipped with Ni-filtered Cu Kα radiation ($\lambda = 0.154$ nm) operating at 40 kV and 40 mA with a fixed slit. The scan rate was 1.0° (2θ) min^{-1} and the scan scope was from 1° to 30° (2θ).

FTIR spectra were obtained with KBr pressed pellet method using a Bruker VERTEX 70 Fourier transform infrared spectrometer. The KBr pellets were prepared by pressing the mixtures of 0.9 mg powder and 80 mg KBr. All spectra were collected at room temperature in the range 4000–400 cm^{-1} with a resolution of 4 cm^{-1} and 64 scans.

TG–DTG was obtained using a NETZSCH STA 409 thermal analyser. The samples were heated with the rate of 10 °C min^{-1} under a flow of high purity nitrogen from 30 to 1000 °C.

Nitrogen adsorption–desorption isotherms were measured on a Micromeritics ASAP 2020M instrument. Before the adsorption tests, the samples were outgassed under vacuum over 12 h at 100 °C. The multiple-point Brunauer–Emmett–Teller (BET) method was used to calculate the specific surface areas of the samples.

The CHN elemental microanalyses were obtained on an Elementar Vario EL III Universal CHNOS Elemental Analyzer. The grafted amount of APTES (M_{APTES}, mol silane g^{-1} sample) was determined by $M_{APTES} = W_N/M_N$, where W_N was the content (wt.%) of nitrogen obtained by CHN analysis in which the content of nitrogen in the original Al_{13}-intercalated/Al-pillared sample at the same temperature had been subtracted. M_N was the molar mass of N (14.007 g mol^{-1}).

3. Results and discussion

3.1. X-ray diffraction

The XRD patterns of Al_{13}-intercalated/Al-pillared montmorillonite samples are shown in Fig. 1a–c. The basal spacing (d_{001}) of Al_{13}-IMt is 1.90 nm (Fig. 1a). The interlayer spacing distance of Al_{13}-IMt (0.94 nm) is consistent with the size (~0.9 nm) of hydroxyaluminum polycation ($[AlO_4Al_{12}(OH)_{24}(OH_2)_{12}]^{7+}$). This is a proof for the successful intercalation of hydroxyaluminum polycation into the interlayer space of montmorillonite.

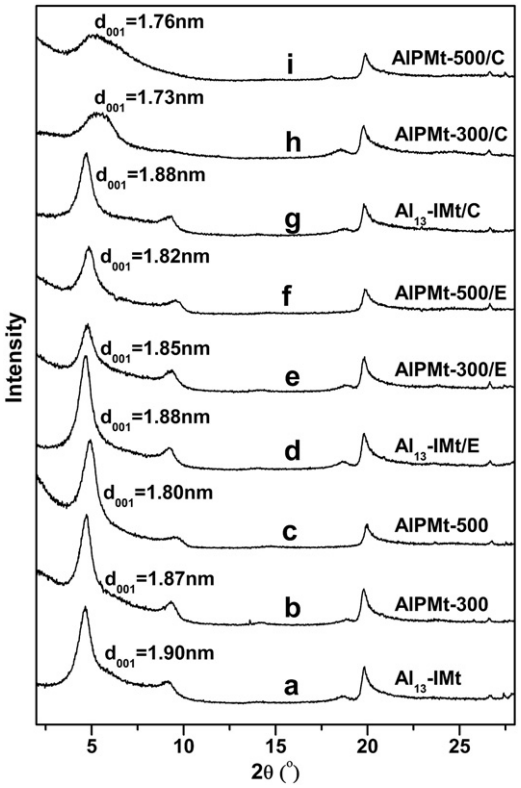

Fig. 1. XRD patterns of the samples before and after APTES modification.

After calcinations, the values of d_{001} are 1.87 nm for AlPMt-300 (Fig. 1b) and 1.80 nm for AlPMt-500 (Fig. 1c), respectively. The interlayer spaces decrease slightly but do not collapse. And the sharp and distinct d_{001} peak shows that the calcined samples still have good degree of crystallinity.

The XRD patterns of the APTES-modified samples are shown in Fig. 1d–f (anhydrous ethanol as solvent) and Fig. 1g–i (cyclohexane as solvent). After modification, the elevation of baseline has been observed, and the peaks of d_{001} become slightly broader than their intercalated/pillared counterpart, especially the ones prepared in cyclohexane. This is attributed to amorphous silicon compounds that exist in the interlayer space. But there are little changes of the position of the peaks. The interlayer spacing distances of the APTES-modified samples prepared in anhydrous ethanol (1.88 nm for Al_{13}-IMt/E, 1.85 nm for AlPMt-300/E, and 1.82 nm for AlPMt-500/E) and Al_{13}-IMt/C (1.88 nm) are closed to their corresponding intercalated/pillared montmorillonite, but AlPMt-300/C (1.73 nm) and AlPMt-500/C (1.76 nm) show some decreases in interlayer spacing distances which may be caused by the little collapses of interlayer structure after long-time stirring and refluxing. These results confirm that the structure of the Al-pillared montmorillonite is mostly retained in the process of APTES modification.

3.2. FTIR spectra

The FTIR spectra of the samples are given in Fig. 2 and the assignments of the peaks (Madejova, 2003; Shanmugharaj et al., 2006; Zhu et al., 2007) are listed in Table 1. The bands of Al_{13}-IMt, AlPMt-300 and AlPMt-500 (Fig. 2a–c) at 3620 cm^{-1} are the stretching vibration of isolated hydroxyl groups bonded to the aluminum or magnesium (Al(Mg)OH or Al(Al)OH), and it is also proved by the bending vibrations of Al(Al)OH at 920 cm^{-1}. The peaks at 3446 and 1631 cm^{-1} are attributed to the –OH stretching and bending vibrations of the adsorbed water, respectively. After calcinations, the intensities of these peaks decrease since the removal of the adsorbed water and the hydroxyl groups. The peaks at 1401 and 845 cm^{-1} are corresponded to the antisymmetrical stretching vibration and in-

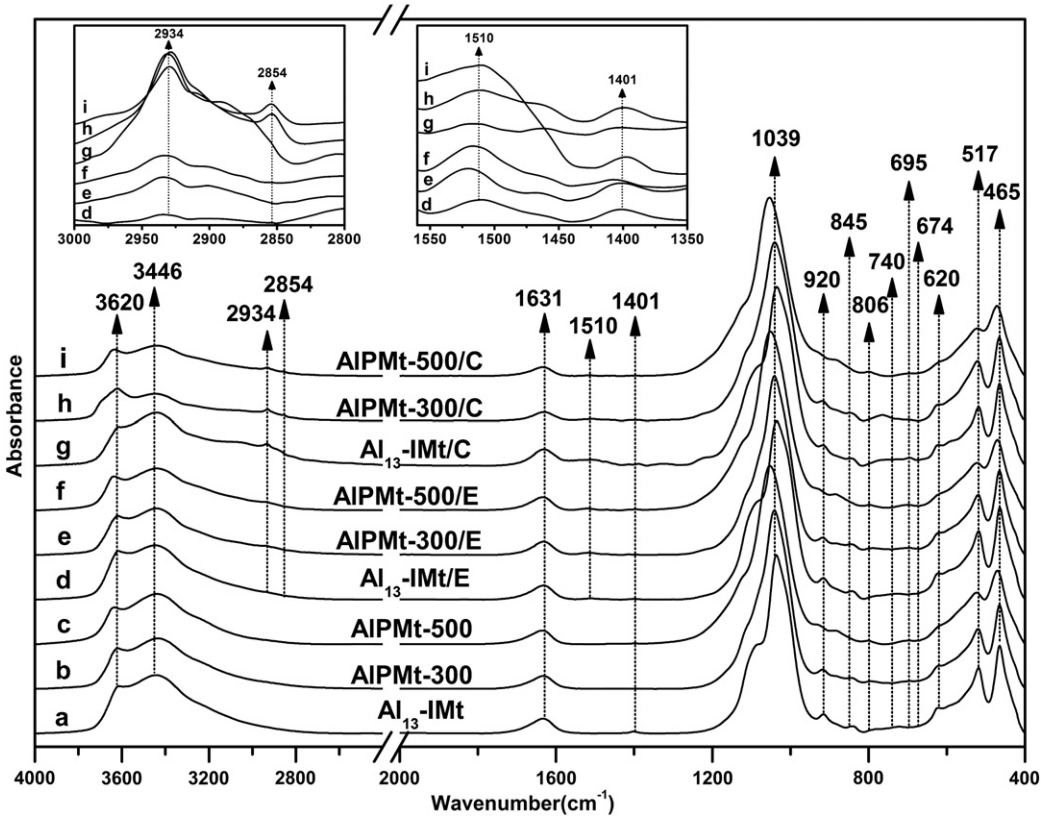

Fig. 2. FTIR spectra of the samples before and after APTES modification.

Table 1
Positions and assignments of the FTIR vibration bands.

Position (cm^{-1})	Assignments	Position (cm^{-1})	Assignments
3620	–OH stretching of Al–OH and Mg–OH	920	–OH deformation of Al^{VI}–OH
3446	–OH stretching of interlayer water	845	In-plane bending of CO_3^{2-}
2934	Antisymmetric stretching of $–CH_2$	806	–OH deformation of Mg^{VI}–OH
2854	Symmetric stretching of $–CH_2$	740	Out-of-plane bending of CO_3^{2-}
1631	–OH deformation of interlayer water	695, 674,	Stretching of Si–O–Si and Si–O–Al
1510	Deformation of $–CH_2$	620	
1401	Antisymmetric stretching of CO_3^{2-}	517	Deformation of Si–O–Al^{VI}
1039	Si–O stretching	465	Deformation of Si–O–Si

plane bending vibration of carbonyl groups, respectively. These groups come from a small amount of carbonates that remained in the samples. With the increase of the calcination temperature, the intensities of these peaks decrease since the decomposition of the carbonates.

The FTIR spectra of the APTES-modified samples are shown in Fig. 2d–i. The new appearing peak at 2934 cm^{-1} and a small peak at 2854 cm^{-1} are attributed to the antisymmetric and symmetric stretching vibrations of $–CH_2$, respectively. And the weak peak at about 1510 cm^{-1} corresponds to the bending vibrations of $–CH_2$. These results are consistent with the research of Shanmugharaj et al. (2006) and confirm the presence of the silane in the samples of these intercalated/pillared montmorillonite. These new peaks of the samples prepared in cyclohexane are more obvious than that in anhydrous ethanol. It implies that the grafting amount of APTES in cyclohexane is larger than that in anhydrous ethanol, which is because the hydrolysis of APTES is restrained in anhydrous ethanol.

For the samples prepared in anhydrous ethanol (Fig. 2d–f), the sequence of the intensities of the peaks at 2934 and 1510 cm^{-1} is AlPMt-300/E>Al_{13}-IMt/E>AlPMt-500/E. This means the loading amounts of APTES in these samples follow the same sequence. The reason is that the structure of the interlayer Al compound gradually transforms from Keggin ions to oxides with the rising temperature, and the amounts of hydroxyl groups in the interlayer Al compounds decrease. For AlPMt-300, only some hydroxyl groups in the interlayer Al compounds are removed by heating, and the Keggin structure was not destroyed. The ethanol molecules can provide protons to compensate the losses of hydroxyls in these interlayer Al compounds. Meanwhile, this compensation effect also facilitates the hydrolysis of APTES because of the consumption of ethanol molecules. Both of these cause the increase of grafting amount. For AlPMt-500, most of the interlayer Al pillars are oxides with different oxidation degrees, the hydroxyl groups in the pillars are obviously less than that Al_{13}-IMt and AlPMt-300, so the grafting amounts decrease. These results also demonstrate that the grafting reaction between APTES and Al_{13}-intercalated/Al-pillared montmorillonite mainly takes place on the surface of the interlayer Al compounds other than the layers of montmorillonite. For the APTES-modified samples prepared in cyclohexane (Fig. 2g–i), the intensities of the peaks at 2934 and 1510 cm^{-1} both decrease with the increasing calcination temperature. And this means the loading amounts of APTES in these samples follow the sequence: Al_{13}-IMt/C>AlPMt-300/C>AlPMt-500/C.

3.3. Thermal analysis

The TG and DTG curves of the samples before and after grafting are shown in Fig. 3. There are two major mass losses in the curves for the samples without modification (Fig. 3a–c). The first one (Loss-M1) happened in the range of 30–300 °C, according to the DTG curve peak at ~100 °C. The corresponding mass losses of Al_{13}-IMt, AlPMt-300 and AlPMt-500 are 14.23, 10.41, and 8.27 wt.%, respectively. These mass losses are attributed to the removal of physisorbed water on the surface and interlayer space of the intercalated/pillared montmorillonite. Because the increasing calcination temperature results in the dehydration in the interlayer space of these intercalated/pillared montmorillonite, so the mass losses of the three samples decrease. The second mass loss (Loss-M2) is taken between 300 and 700 °C, which are in the light of the DTG curve peaks at ~500 °C for Al_{13}-IMt and AlPMt-300, and 577 °C for AlPMt-500. The mass losses are 8.92% for Al_{13}-IMt, 8.96% for AlPMt-300, and 4.62% for AlPMt-500. These mass losses are due to the dehydroxylation of interlayer Al compounds and octahedron layers in montmorillonite. For Al_{13}-IMt and AlPMt-300, the dehydroxylation of the interlayer Al compounds takes place between 350 and 500 °C, overlapping with the dehydroxylation temperature of the layers of montmorillonite, so the mass losses of these peaks appear at ~500 °C. The hydroxyl groups of Al Keggin structure are mostly decomposed after calcination at 500 °C, so the second mass loss of AlPMt-500 is mainly attributed to the dehydroxylation of montmorillonite layers. Because dehydroxylation temperature of montmorillonite layer is higher than that of Al Keggin structure, the second DTG peak of AlPMt-500 is located at a higher temperature than the other two.

There are three mass losses for most of the APTES-modified samples (taking AlPMt-500/E as an example, Fig. 3f). The mass loss in the range of 30–300 °C (Loss-1), which is 7.09%, is attributed to the removal of physically adsorbed water and/or APTES. This physically adsorbed APTES decomposes at a low temperature because of its worse thermal stability compared with the covalent-bonded APTES. The mass loss in the range of 300–500 °C (Loss-2) is due to the decomposition of grafted silane and dehydroxylation of Al pillars, and the value is 3.68%. The mass loss in the range of 500–700 °C (Loss-3), which corresponds to the DTG peak at 568.7 °C, is attributed to the decomposition of hydroxyl groups in the octahedron layer of montmorillonite, and the value is 3.51%.

The mass losses at 30–300 °C of the APTES-modified samples are smaller than those of the unmodified intercalated/pillared montmorillonite samples. Because the silanes enter into the interlayer space and replace the water molecules, the water contents of the APTES-modified samples decrease. The mass losses of these APTES-modified samples at 300–700 °C are higher than that of the unmodified ones, and the increments result from the decomposition of APTES. For Al_{13}-IMt/C, Al_{13}-IMt/E, AlPMt-300/C and AlPMt-300/E, there is a broad DTG peak at 300–700 °C, since APTES and hydroxyl groups of Al pillars both decompose at ~400 °C and the two DTG peaks overlap to form a strong broad peak which conceals the peak caused by the dehydroxylation of montmorillonite. For AlPMt-500/E and AlPMt-500/C, there are two DTG peaks between 300 and 700 °C, because there is a discrepancy between the decomposing temperature of APTES and the hydroxyl groups in montmorillonite. Comparing the mass losses at 30–500 °C of the APTES-modified samples (Table 2), which relatively present the APTES grafting amounts of the samples pretreated with the same calcination temperature, and it follows the orders as Al_{13}-IMt/C>Al_{13}-IMt/E, AlPMt-300/C>AlPMt-300/E, and AlPMt-500/C>AlPMt-500/E. And this is also proved by the results of FTIR.

3.4. Elemental analysis

The percentages of nitrogen (wt.%) in the results of elemental analysis are chosen for the calculation of the contents of grafted APTES. The results are listed in Table 2. The maximum grafted amount is 2.02 mmol g^{-1} for Al_{13}-IMt/C, and the minimum amount is 0.23 mmol g^{-1} in AlPMt-500/E. At the same calcination temperature, the grafted amounts of the samples prepared in cyclohexane are all greater than that in anhydrous ethanol. It is consistent with the result

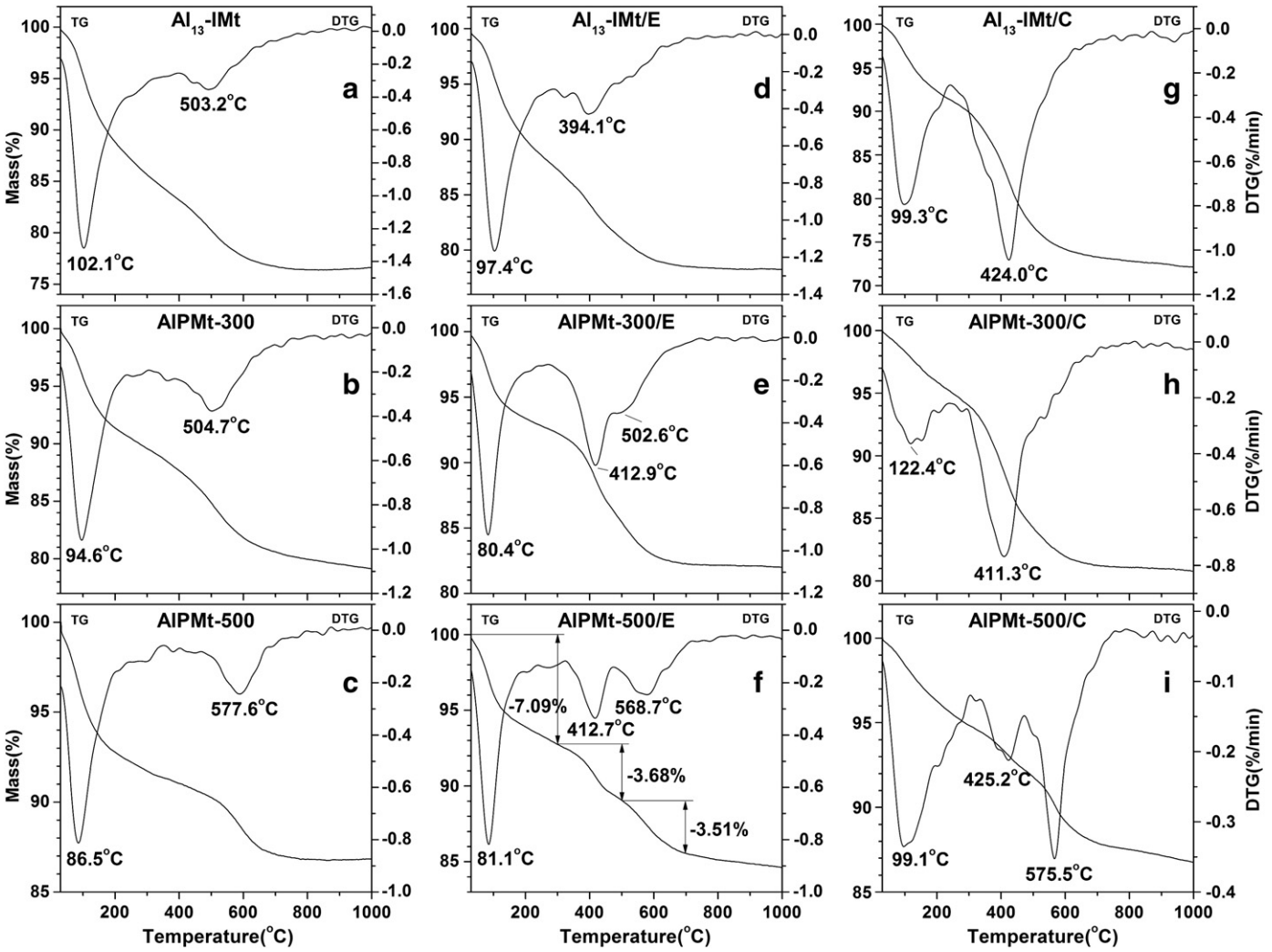

Fig. 3. TG and DTG curves of the samples before and after APTES modification.

of FTIR that the peaks at 2934 cm^{-1} of the samples prepared in cyclohexane are more obvious than that in anhydrous ethanol, and the results of TG–DTG about comparing the grafting amounts of the samples. This is because the products of hydrolysis of APTES contain ethanol, so the reaction in anhydrous ethanol is restrained. We also find that, with the increase of calcination temperature, the grafting amount in anhydrous ethanol firstly increases then decreases. There are two reasons for this phenomenon. First, the hydroxyl groups of interlayer Al compounds decrease with the increasing temperature. When the temperature is 300 °C, some hydroxyl groups in pillared montmorillonite are lost, but the hydroxyl groups in ethanol molecules provide protons for compensation. These protons bond with the broken bonds of Al compounds and clay layers, forming new hydroxyls. This compensates the hydroxyl losses caused by calcination and results in new grafting amounts in the samples prepared by AlPMt-300. Second, the consumption of ethanol around the reactive sites facilitates the hydrolysis of APTES and promotes the occurrence of silylation. So the grafting amounts of AlPMt-300/E are more than Al_{13}-IMt/E. When the calcination temperature is higher (500 °C), the Keggin structures of the interlayer Al compounds were transformed into oxides. The amounts of hydroxyls reduce sharply, leading to the decrease of grafted amounts. This also proves that APTES molecules mainly react with the hydroxyl groups of Al pillars, other than the broken bonds of the phyllisilicate layers. But for the samples prepared in cyclohexane, the grafted amounts decrease with the increasing temperature, since the cyclohexane molecules are stable and do not provide protons for compensation.

Table 2
Data of thermogravimetric analysis and elemental analysis.

Sample	Mass loss[a]	Nitrogen content[b]	Grafted amount[c]
Al_{13}-IMt/C	23.17	2.83	2.02
Al_{13}-IMt/E	18.96	0.39	0.28
AlPMt-300/C	15.71	1.05	0.75
AlPMt-300/E	14.31	0.91	0.65
AlPMt-500/C	10.77	0.38	0.27
AlPMt-500/E	8.91	0.32	0.23

[a] Mass losses (wt.%) of the grafted samples between 30 and 500 °C by thermogravimetric analysis.
[b] Nitrogen contents (wt.%) of the grafted samples through elemental analysis.
[c] APTES grafted amounts of the APTES-modified samples (mmol APTES g^{-1} sample).

3.5. Nitrogen adsorption–desorption isotherms

The nitrogen adsorption and desorption isotherms of the Al_{13}-intercalated/Al-Pillared montmorillonite samples, and the grafted samples prepared in anhydrous ethanol and cyclohexane are shown in Fig. 4. The adsorption isotherms of the samples are all of type IV.

For Al_{13}-IMt, AlPMt-300 and AlPMt-500, the nitrogen quantity adsorbed increases with the calcination temperature. This is also proved by the specific surface areas calculated with BET method and the total pore volumes (Fig. 5). For Al_{13}-IMt, they are 209 m^2 g^{-1} and

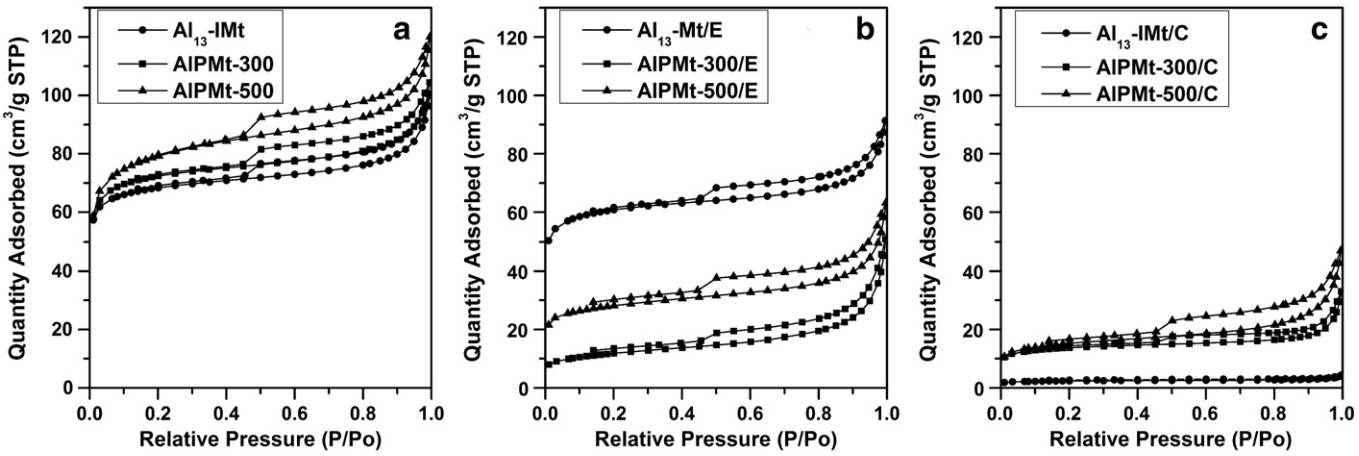

Fig. 4. Nitrogen adsorption–desorption isotherms of the samples before and after APTES modification.

0.155 $m^3\ g^{-1}$. After calcinations, they are 222 $m^2\ g^{-1}$ and 0.161 $m^3\ g^{-1}$ for AlPMt-300, and 247 $m^2\ g^{-1}$ and 0.186 $m^3\ g^{-1}$ for AlPMt-500. With the increasing calcination temperature, dehydroxylation of the pillars takes place, and the interlayer compounds transform from Al polycations to compact oxides and occupy smaller interlayer space. This will change the structure of some micropores. But the interlayer structure does not collapse with the increasing temperature, which is deduced from the little changes of interlayer space distances according to the XRD results. So there is a little increment of interlayer space after calcinations.

For the APTES-modified samples prepared in anhydrous ethanol, Al_{13}-IMt/E has the highest BET specific surface area and total pore volume among the APTES-modified samples, which are 160 $m^2\ g^{-1}$ and 0.134 $m^3\ g^{-1}$. This suggests that Al_{13}-IMt/E still keeps a big specific surface area and pore structure, which is helpful for its application as absorbents. The specific surface areas and total pore volumes of AlPMt-300/E and AlPMt-500/E are 39 $m^2\ g^{-1}$ and 0.079 $m^3\ g^{-1}$, 89 $m^2\ g^{-1}$ and 0.098 $m^3\ g^{-1}$ respectively. It means that there are more grafting amounts in these samples than Al_{13}-IMt/E, and AlPMt-300 is easier to react with APTES than AlPMt-500 in anhydrous ethanol.

The APTES-modified samples prepared in cyclohexane all have very small specific surface areas and total pore volumes, especially Al_{13}-IMt/C, whose specific surface area and total pore volume are only 7 $m^2\ g^{-1}$ and 0.007 $m^3\ g^{-1}$, respectively. These also demonstrate large grafting amounts in these samples and the pore structure is blocked by silane molecules. These results are also in accordance with the results of FTIR spectra and the grafted amounts calculated by the data of element analysis.

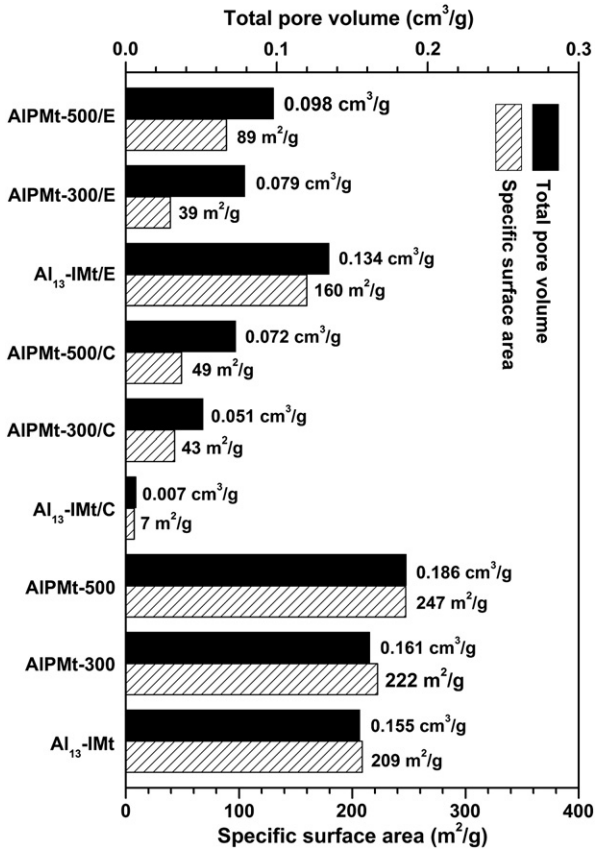

Fig. 5. BET specific surface areas and total pore volumes of the APTES-modified sample.

3.6. Modification mechanism of Al_{13}-intercalated/Al-pillared montmorillonite with APTES

Three types of reactive sites for grafting may exist in Al_{13}-intercalated/Al-pillared montmorillonite: the surface of interlayer Al Keggin ions and/or Al oxides with hydroxyls (Zhu et al., 2007), the edges (external surfaces) of the tetrahedral layers of montmorillonite (Bourlinos et al., 2004), and the interlayer surfaces of montmorillonite which have silanol groups caused by isomorphous substitution (He et al., 2005). By analyzing the APTES-modified samples with pretreatments at different temperatures, we find that grafting mainly occurs between the hydrolyzed APTES and the hydroxyl groups of the interlayer Al compounds. Keggin structure of interlayer compounds is not destroyed after calcination at 300 °C, and the grafting amounts of these calcined samples do not decrease compared with that of their counterparts which are not calcined. After calcination at 500 °C, Keggin structure is essentially destroyed, and we observe that the grafting amounts decrease significantly.

By analyzing the grafting amounts derived from the elemental analysis and the specific surface areas, we also find that the formation processes of the final products in anhydrous ethanol and cyclohexane have some differences. There are two steps, hydrolysis and grafting, in the APTES-modified Al_{13}-intercalated/Al-pillared montmorillonite in anhydrous ethanol. However, there are three steps, hydrolysis, grafting and oligomerization, in the cyclohexane system.

For the samples prepared in anhydrous ethanol, the extent of grafting is relatively low, so the interlayer porous structure is greatly retained (taking Al_{13}-IMt/E as an example, Fig. 6a). That is because the hydrolysis products of APTES contain ethanol, and the hydrolysis of APTES is restrained in anhydrous ethanol. Moreover, anhydrous ethanol is a kind of polar solvent which contains hydroxyl groups. The

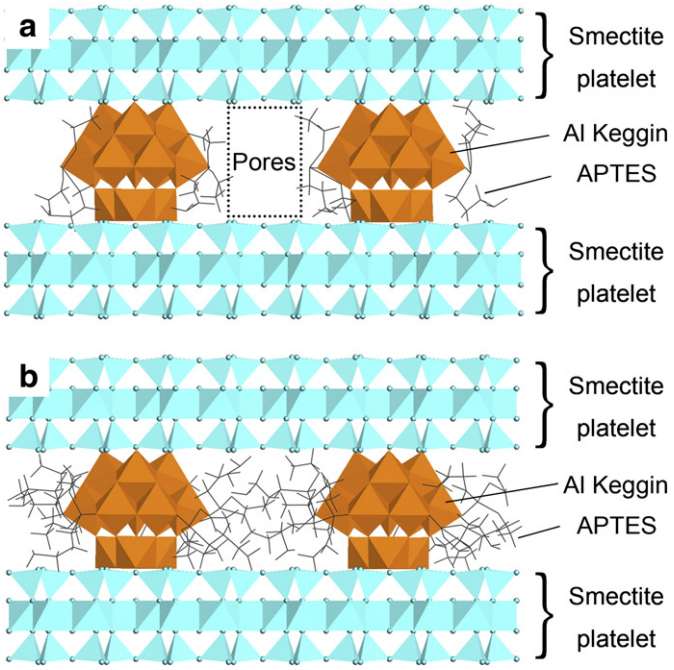

Fig. 6. Schematic representation of the structure of the APTES-modified samples: (a) low extent of APTES grafting to retain the interlayer pore structure (prepared in anhydrous ethanol), taking Al_{13}-IMt/E as an example; (b) high extent of APTES grafting to block the interlayer pores (prepared in cyclohexane), taking Al_{13}-IMt/C as an example.

interactions between APTES and ethanol are strong and these are not favorable for the reaction of grafting. So there are little grafting amounts of these samples prepared in anhydrous ethanol.

In contrast with that, the cyclohexane has little interaction with APTES, and more APTES molecules are hydrolyzed into silanols. These silanols interact with the hydroxyl groups on the surface of Al Keggin ion/Al oxides, forming stable covalent bonds. Moreover, some of the silanol molecules are inclined to condense with each other making amorphous oligomerized products and this blocking the pore structure of Al_{13}-intercalated/Al-pillared montmorillonite. So there is a large grafting amount of APTES in the interlayer space (taking Al_{13}-IMt/C as an example, Fig. 6b).

These results illustrate that the porous structure of APTES-modified Al_{13}-intercalated/Al-pillared montmorillonite is adjusted by controlling the temperature of pretreatment and choosing the solvent. According to the current information, the modification in anhydrous ethanol without pretreatments is more favorable for maintaining the porous structure. It is postulated that this organo-modified Al_{13}-intercalated/Al-pillared montmorillonite with a porous structure has a potential application in the adsorption of organic pollutants. The relevant work is under way.

4. Conclusions

3-Aminopropyltriethoxysilane (APTES) has been successfully grafted onto the Al_{13}-intercalated/Al-pillared montmorillonite. The grafting reactions mainly take place on the surface of interlayer Al compounds with hydroxyl groups. The mechanisms of modification are different when using different solvents and include not only the direct grafting of APTES but also oligomerization, in which the hydrolyzed APTES condensed with each other to form a cross-linked structure. The products with different grafted amounts are prepared by controlling the experimental conditions. The APTES functionalized Al_{13}-IMt prepared in anhydrous ethanol (Al_{13}-IMt/E) has the largest specific surface area (~160 $m^2\,g^{-1}$), and the one (Al_{13}-IMt/C) with the maximum loading amount of silane (2.02 $mmol\,g^{-1}$) was obtained in cyclohexane. Thermal treatment not only reduces the water contents of the Al_{13}-intercalated/Al-pillared montmorillonite, but also causes the transformation of the interlayer Al compounds from polycations to oxides. The final loading amount depends on both of these effects. The porous structure can be adjusted by choosing the solvents and the pretreatment conditions. These hybrid organic–inorganic materials enable extensive applications in environmental restoration, especially for the removal of organic pollutants by adsorption.

Acknowledgements

This work was financially supported by the National Science Fund for Distinguished Young Scholars (Grant No. 40725006) and the National Natural Science Foundation of China (Grant No. U0933003). This is contribution No. IS-1249 from GIGCAS.

References

Alkaram, U.F., Mukhlis, A.A., Al-Dujaili, A.H., 2009. The removal of phenol from aqueous solutions by adsorption using surfactant-modified bentonite and kaolinite. J. Hazard. Mater. 169 (1–3), 324–332.
Baskaralingam, P., Pulikesi, M., Elango, D., Ramamurthi, V., Sivanesan, S., 2006. Adsorption of acid dye onto organobentonite. J. Hazard. Mater. 128 (2–3), 138–144.
Bergaya, F., Lagaly, G., 2001. Surface modification of clay minerals. Appl. Clay Sci. 19 (1–6), 1–3.
Bhattacharyya, K.G., Sen Gupta, S., 2008. Adsorption of a few heavy metals on natural and modified kaolinite and montmorillonite: a review. Adv. Colloid Interface Sci. 140 (2), 114–131.
Bourlinos, A.B., Jiang, D.D., Giannelis, E.P., 2004. Clay-organosiloxane hybrids: a route to cross-linked clay particles and clay monoliths. Chem. Mater. 16 (12), 2404–2410.
Carrado, K.A., Xu, L.Q., Csencsits, R., Muntean, J.V., 2001. Use of organo- and alkoxysilanes in the synthesis of grafted and pristine clays. Chem. Mater. 13 (10), 3766–3773.
Chae, H.J., Nam, I.S., Ham, S.W., Hong, S.B., 2001. Physicochemical characteristics of pillared interlayered clays. Catal. Today 68 (1–3), 31–40.
Chen, Q.Q., Wu, P.X., Li, Y.Y., Zhu, N.W., Dang, Z., 2009. Heterogeneous photo-Fenton photodegradation of reactive brilliant orange X-GN over iron-pillared montmorillonite under visible irradiation. J. Hazard. Mater. 168 (2–3), 901–908.
Cheng, M.M., Song, W.J., Ma, W.H., Chen, C.C., Zhao, J.C., Lin, J., Zhu, H.Y., 2008. Catalytic activity of iron species in layered clays for photodegradation of organic dyes under visible irradiation. Appl. Catal. B Environ. 77 (3–4), 355–363.
Daniel, L.M., Frost, R.L., Zhu, H.Y., 2008. Edge-modification of laponite with dimethyloctylmethoxysilane. J. Colloid Interface Sci. 321 (2), 302–309.
de Paiva, L.B., Morales, A.R., Diaz, F.R.V., 2008. Organoclays: properties, preparation and applications. Appl. Clay Sci. 42 (1–2), 8–24.
Ding, Z., Kloprogge, J.T., Frost, R.L., Lu, G.Q., Zhu, H.Y., 2001. Porous clays and pillared clays-based catalysts. Part 2: a review of the catalytic and molecular sieve applications. J. Porous Mater. 8 (4), 273–293.
Gonzalez, F., Pesquera, C., Benito, I., Herrero, E., Poncio, C., Casuscelli, S., 1999. Pillared clays: catalytic evaluation in heavy oil cracking using a microactivity test. Appl. Catal. A Gen. 181 (1), 71–76.
He, H.P., Duchet, J., Galy, J., Gerard, J.F., 2005. Grafting of swelling clay materials with 3-aminopropyltriethoxysilane. J. Colloid Interface Sci. 288 (1), 171–176.
Herrera, N.N., Letoffe, J.M., Putaux, J.L., David, L., Bourgeat-Lami, E., 2004. Aqueous dispersions of silane-functionalized laponite clay platelets. A first step toward the elaboration of water-based polymer/clay nanocomposites. Langmuir 20 (5), 1564–1571.
Itadani, A., Tanaka, M., Abe, T., Taguchi, H., Nagao, M., 2007. Al-pillared montmorillonite clay minerals: low-pressure CO adsorption at room temperature. J. Colloid Interface Sci. 313 (2), 747–750.
Jiang, J.Q., Cooper, C., Ouki, S., 2002. Comparison of modified montmorillonite adsorbents — part I: preparation, characterization and phenol adsorption. Chemosphere 47 (7), 711–716.
Kloprogge, J.T., 1998. Synthesis of smectites and porous pillared clay catalysts: a review. J. Porous Mat. 5 (1), 5–41.
Lagaly, G., 1986. Interaction of alkylamines with different types of layered compounds. Solid State Ionics 22 (1), 43–51.
Liu, P., 2007. Polymer modified clay minerals: a review. Appl. Clay Sci. 38 (1–2), 64–76.
Liu, X.D., Lu, X.C., 2006. A thermodynamic understanding of clay-swelling inhibition by potassium ions. Angew. Chem. Int. Ed. 45 (38), 6300–6303.
Madejova, J., 2003. FTIR techniques in clay mineral studies. Vib. Spectrosc. 31 (1), 1–10.
Malani, A., Ayappa, K.G., Murad, S., 2009. Influence of hydrophilic surface specificity on the structural properties of confined water. J. Phys. Chem. B 113 (42), 13825–13839.
Martinez-Ortiz, M.J., Fetter, G., Dominguez, J.M., Melo-Banda, J.A., Ramos-Gomez, R., 2003. Catalytic hydrotreating of heavy vacuum gas oil on Al- and Ti-pillared clays prepared by conventional and microwave irradiation methods. Microporous Mesoporous Mater. 58 (2), 73–80.
Occelli, M.L., Bertrand, J.A., Gould, S.A.C., Dominguez, J.M., 2000. Physicochemical characterization of a Texas montmorillonite pillared with polyoxocations of

aluminum: part I: the microporous structure. Microporous Mesoporous Mater. 34 (2), 195–206.
Okada, A., Usuki, A., 2006. Twenty years of polymer-clay nanocomposites. Macromol. Mater. Eng. 291 (12), 1449–1476.
Pinnavaia, T.J., 1983. Intercalated clay catalysts. Science 220 (4595), 365–371.
Pires, J., Bestilleiro, M., Pinto, M., Gil, A., 2008. Selective adsorption of carbon dioxide, methane and ethane by porous clays heterostructures. Sep. Purif. Technol. 61 (2), 161–167.
Ruiz-Hitzky, E., Meerbeek, A.V., 2006. Clay mineral- and organoclay-polymer nanocomposite. In: Bergaya, F., Theng, B.K.G., Lagaly, G. (Eds.), Handbook of Clay Science. Elsevier Science, Amsterdam.
Sanchez-Martin, M.J., Rodriguez-Cruz, M.S., Andrades, M.S., Sanchez-Camazano, M., 2006. Efficiency of different clay minerals modified with a cationic surfactant in the adsorption of pesticides: influence of clay type and pesticide hydrophobicity. Appl. Clay Sci. 31 (3–4), 216–228.
Shanmugharaj, A.M., Rhee, K.Y., Ryu, S.H., 2006. Influence of dispersing medium on grafting of aminopropyltriethoxysilane in swelling clay materials. J. Colloid Interface Sci. 298 (2), 854–859.
Shimizu, K.I., Kaneko, T., Fujishima, T., Kodama, T., Yoshida, H., Kitayama, Y., 2002. Selective oxidation of liquid hydrocarbons over photoirradiated TiO_2 pillared clays. Appl. Catal. A Gen. 225 (1–2), 185–191.
Tunega, D., Benco, L., Haberhauer, G., Gerzabek, M.H., Lischka, H., 2002. Ab initio molecular dynamics study of adsorption sites on the (001) surfaces of 1:1 dioctahedral clay minerals. J. Phys. Chem. B 106 (44), 11515–11525.
Wheeler, P.A., Wang, J.Z., Baker, J., Mathias, L.J., 2005. Synthesis and characterization of covalently functionalized laponite clay. Chem. Mater. 17 (11), 3012–3018.
Wu, P.X., Wu, W.M., Li, S.Z., Xing, N., Zhu, N.W., Li, P., Wu, J.H., Yang, C., Dang, Z., 2009. Removal of Cd^{2+} from aqueous solution by adsorption using Fe-montmorillonite. J. Hazard. Mater. 169 (1–3), 824–830.
Xi, Y.F., Frost, R.L., He, H.P., 2007. Modification of the surfaces of Wyoming montmorillonite by the cationic surfactants alkyl trimethyl, dialkyl dimethyl, and trialkyl methyl ammonium bromides. J. Colloid Interface Sci. 305 (1), 150–158.
Yang, R.T., Baksh, M.S.A., 1991. Pillared clays as a new class of sorbents for gas separation. AIChE J. 37 (5), 679–686.
Yuan, P., He, H.P., Bergaya, F., Wu, D.Q., Zhou, Q., Zhu, J.X., 2006. Synthesis and characterization of delaminated iron-pillared clay with meso-microporous structure. Microporous Mesoporous Mater. 88 (1–3), 8–15.
Yuan, P., Southon, P.D., Liu, Z.W., Green, M.E.R., Hook, J.M., Antill, S.J., Kepert, C.J., 2008. Functionalization of halloysite clay nanotubes by grafting with gamma-aminopropyltriethoxysilane. J. Phys. Chem. C 112 (40), 15742–15751.
Zhu, L.Z., Tian, S.L., Zhu, H.X., Shi, Y., 2007. Silylated pillared clay (SPILC): a novel bentonite-based inorgano-organo composite sorbent synthesized by integration of pillaring and silylation. J. Colloid Interface Sci. 315 (1), 191–199.
Zhu, J.X., Yuan, P., He, H.P., Frost, R., Tao, Q., Shen, W., Bostrom, T., 2008a. In situ synthesis of surfactant/silane-modified hydrotalcites. J. Colloid Interface Sci. 319 (2), 498–504.
Zhu, J.X., Zhu, L.Z., Zhu, R.L., Chen, B.L., 2008b. Microstructure of organo-bentonites in water and the effect of steric hindrance on the uptake of organic compounds. Clays Clay Miner. 56 (2), 144–154.
Zhu, R.L., Wang, T., Ge, F., Chen, W.X., You, Z.M., 2009a. Intercalation of both CTMAB and Al_{13} into montmorillonite. J. Colloid Interface Sci. 335 (1), 77–83.
Zhu, R.L., Zhu, J.X., Ge, F., Yuan, P., 2009b. Regeneration of spent organoclays after the sorption of organic pollutants: a review. J. Environ. Manag. 90 (11), 3212–3216.